Preprints of the 23rd IFAC World Congress
Busan, Republic of Korea, August 23-28, 2026

A Cepstrum-based, Vehicle- and Speed-independent Road Roughness Index from Inertial Sensor Data

Simone Gelmini *
Jessica Leoni ** **Marco Centurioni** ** **Nicola Pivaro** **
Silvia Strada ** **Mara Tanelli** ** **Sergio M. Savaresi** **

* *Department of Mechanical Engineering - Massachusetts Institute of Technology, 77 Massachusetts Ave, Cambridge, MA, 02139, United States (affiliation at the time this study was conducted). (e-mail: gelmini@mit.edu)*
** *Dipartimento di Elettronica, Informazione e Bioingegneria, Politecnico di Milano, 20133 Milan, Italy (e-mail:{jessica.leoni, marco.centurioni, nicola.pivaro, silvia.strada, mara.tanelli, sergio.savaresi}@polimi.it).*

Abstract: Objective road quality estimation is essential for smart infrastructure. Using everyday vehicles with low-cost inertial sensors provides a cost-effective and scalable solution. However, vertical acceleration signals are influenced by vehicle dynamics and speed, producing biased estimates. This issue has been addressed by proposing a novel approach that, using cepstral analysis, separates road-induced and vehicle behaviors. Specifically, thanks to a one-time, model-free calibration, it identifies the latter, providing an unbiased estimate of the first. Last, cepstral features also provide robustness to speed. Validation with naturalistic data across vehicles, drivers, and roads demonstrates accuracy and robustness, highlighting its potential for large-scale road monitoring.

Keywords: Modeling and supervision of automotive systems; Road-quality estimation; Data-driven identification; Decision support system in transportation; Signal processing and analysis

1. PROBLEM DESCRIPTION AND RELATED WORKS

Road infrastructure is essential not only to support economic opportunities but also to promote traffic safety, and reduce vehicle wear and usage, thus ensuring adequate transport standards for any user Braghin et al. (2006). However, achieving this goal is highly ambitious and demanding, as it requires timely maintenance that, in turn, needs continuous road condition monitoring.

To address this problem, research has focused on continuous road monitoring approaches compatible with limited financial resources. This led to a range of solutions that can be grouped into three categories:

- direct road profile measuring instruments,
- visual inspection tools,
- vehicle dynamics measuring sensors.

The first category includes instruments such as profilometers, which reconstruct the road profile independently of vehicle type or driving behavior Spangler and Kelly (1965). However, their high cost limits installation to a few vehicles, hindering scalability and continuous monitoring. The second category consists of visual inspection tools, such as cameras mounted on vehicles or drones, and satellite imagery, which generate 2D or 3D reconstructions of the road surface Yiliguoqi et al. (2026). Despite their accuracy, these methods remain expensive, unsuitable for continuous monitoring, and sensitive to adverse weather conditions. As a result, the third category emerged as the most promising, which uses the vehicle itself as a mobile sensor. In practice, according to these approaches, road quality is estimated using physics-based or data-driven techniques. The former requires detailed knowledge of parameters such as vehicle mass, tyre condition, and suspension characteristics, often implying additional sensors. Given these inputs, they can achieve high accuracy using traditional methods, e.g., International Roughness Index (IRI), or more sophisticated alternatives such as adaptive observers or power spectral analysis Zhang et al. (2022). However, their hardware requirements limit scalability and conflict with easy instrumentation and retrofitting. The second group, increasingly dominant, proposes data-driven solutions that do not require explicit knowledge of vehicle parameters. These methods leverage low-cost sensor boxes, widely used in the automotive insurance sector, typically integrating an IMU and a GPS/GNSS module, which provide effective data for continuous vehicle dynamics monitoring. Indicators in this context mainly rely on the energy content of the vertical acceleration signal, as a proxy for energy transferred from road irregularities to the vehicle body. To this end, frequency-based and time-based indices have been proposed; the former exploit the power spectral density, inspired by ISO 8608, while the latter use time-domain statistics such as the Root Mean Square (RMS) Wage and Sester (2021).

So, from the presented literature analysis, it is possible to conclude that vehicle dynamics–based approaches are the most scalable and suitable for continuous monitoring of road conditions. Among them, data-driven methods are the most promising as they provide accurate estimates using low-cost sensors. However, literature approaches are still affected by a common limitation, i.e., they interpret increased excitation along the vertical as an indicator of degraded pavement conditions. This assumption introduces critical biases in the estimate due to the peculiarities of the specific vehicle and its traveling speed. In other words, the measured signals are related to the vehicle–road interaction system, where vehicle dynamics and speed act as filtering mechanisms on the contribution of the actual speed profile. As a result, estimates obtained under different vehicles or operating conditions are generally not directly comparable, as confirmed by experimental studies highlighting significant variability in cross-vehicle and cross-speed scenarios Loprencipe et al. (2019). These limitations motivate the need for methodologies capable of decoupling road-induced excitations from vehicle dynamics, ensuring robustness and consistency across heterogeneous acquisition conditions.

Therefore, this work proposes a novel data-driven approach for continuously estimating road quality, which leads to the definition of the so-called Roughness Profile Index (RPI), which is insensitive to the specific vehicle dynamics and its longitudinal

©2026 the authors. Accepted by IFAC for publication under a Creative Commons Licence CC-BY-NC-ND

speed. The whole approach has been designed to be compliant with large-scale implementation by only requiring a reduced set of measurements from a cost-effective sensor setup, consisting of an accelerometer and a GPS/GNSS unit. This key result is achieved by basing the index formulation on cepstral analysis of the vertical acceleration signal, rather than relying on time- or frequency-domain analyses, commonly adopted in the literature. Specifically, cepstrum, already used to identify system faults in mechanical systems, Randall (2017), has been key as it enables clear identification of the vehicle's dynamics, which can then be filtered out from subsequent acquisitions. Thus, it allows isolating the road-induced dynamics, without requiring any a priori knowledge of the vehicle parameters. Second, being inherently resilient to signal scaling and time warping, it ensures stability under changing traveling speed, Bonnardot (2019). The approach is experimentally validated using preliminary data collected over more than 200 km on diverse road sections, including highway, urban, and off-road environments, at varying speeds and with different drivers. Furthermore, to better underline the advantages of the vehicle dynamics and speed-independent index, an ablation study has been performed to highlight the importance of debiasing the estimate from these factors. In addition, the proposed formulation has been compared to an alternative version based on the power spectrum content of the acceleration signal, which is commonly used by most state-of-the-art approaches.

2. METHODOLOGY

2.1 Cepstral Analysis

The cepstrum was first introduced in Bogert (1963) as an alternative to the autocorrelation function. In this work, power cepstrum formulation has been leveraged; thus, the terms *cepstrum* and *power cepstrum* will be used interchangeably. Given a stationary stochastic process, $p(t)$, whose power spectrum is $\phi_p(\omega)=|P(\omega)|^2$, its cepstrum $c_p(q)$ can be defined as:

$$c_p(q)=\mathcal{F}^{-1}\{\log(\phi_p(\omega))\}, \tag{1}$$

where q is the quefrency variable. It is worth mentioning that this cepstrum formulation is based on a time representation of the process, but the same considerations apply if the process is expressed in the spatial domain.

The idea of basing the proposed methodology on power cepstrum, rather than the more commonly used power spectrum, is motivated by one of its key properties: the power cepstrum of two processes convolved in the time domain corresponds to the sum of their power cepstra in the quefrency domain. This property is, in fact, useful for decoupling vehicle and road dynamics. To better understand the advantage of this property, let us consider a process $p(t)$ defined as the convolution of two distinct processes $p_1(t)$ and $p_2(t)$ as is the case with vertical acceleration measured by the vehicle accelerometer, which is the convolution of the vertical dynamics of the vehicle's itself and the acceleration induced by the road profile. In the time domain, this relationship can be expressed as $p(t)=p_1(t)*p_2(t)$. Given the convolution theorem and the properties of the Fourier transform, the power spectral density of $p(t)$ can be defined as:

$$\phi_p(\omega)=|P(\omega)|^2=|P_1(\omega)\cdot P_1(\omega)|^2=\phi_{p_1}(\omega)\cdot\phi_{p_2}(\omega), \tag{2}$$

where $P_i(\omega)$ and $\phi_{p_i}(\omega)$ are the Fourier transform and the power spectrum of the i_{th} process, respectively. It follows that, based on Equation (1), the power cepstrum of $\phi_p(\omega)$ becomes:

$$\begin{aligned} c_p(q)&=\mathcal{F}^{-1}\{\log(\phi_p(\omega))\}\\ &=\mathcal{F}^{-1}\{\log(\phi_{p_1}(\omega)\cdot\phi_{p_2}(\omega))\}\\ &=\mathcal{F}^{-1}\{\log(\phi_{p_1}(\omega))\}+\mathcal{F}^{-1}\{\log(\phi_{p_2}(\omega))\}\\ &=c_{p_1}(q)+c_{p_2}(q). \end{aligned} \tag{3}$$

This result is key for the methodology proposed in this work, as it provides proxy of the road pavement quality by computing the power cepstrum of the measured acceleration, and then subtracting from it an estimate of the power cepstrum of the vehicle vertical dynamics.
To compute a cepstral difference, the Martin distance δ is employed, Martin (2002), which is defined as:

$$\delta(c_{p_1}(q),c_{p_2}(q))=\sqrt{\sum_{q=0}^{\infty}q|c_{p_1}(q)-c_{p_2}(q)|^2}. \tag{4}$$

This metric is widely used to compute cepstral differences because it effectively captures statistically significant variations, even when applied to the first cepstral coefficients only. This allows for approximating the true Martin distance using only the first Q cepstral terms, making the computation manageable and efficient.

2.2 Vehicle Dynamics Definition

The assumed consists of a second-order single-mass quarter-car, as widely used in the literature due to its ability to accurately capture vehicle behavior by combining the sprung and unsprung masses into a single lumped system:

$$M\ddot{z}(t)+\xi\dot{z}(t)+k(z(t)-z_r(t))=0. \tag{5}$$

In this dynamical equation, $z(t)$ denotes the vertical displacement of the overall system, and $z_r(t)$ represents the height of the road profile. In addition, M is the equivalent mass of the quarter car, whereas k, and ξ are the stiffness of the suspension spring and the damping coefficient, respectively. Note that $\ddot{z}(t)$ corresponds to the overall vertical acceleration of the vehicle, which can also be defined as $a_z(t)$, that is, the one that can be measured by an onboard accelerometer. Thus, the signal $\ddot{z}(t)$ is given by the convolution of the dynamic response of the vehicle and the excitation due to road irregularities.

Although Equation (5) is defined in the time domain, road quality estimation is typically performed in spatial coordinates. This transformation can be performed by assuming quasi-stationarity of the system. Under this assumption, time-domain dynamics can be translated into the spatial domain by applying the change of variables $t=\frac{x}{v}$, where v is the longitudinal velocity of the vehicle, which, thanks to the stationarity assumption, can be considered constant. Based on this transformation, the time derivatives in Equation (5) can be expressed in spatial coordinates:

$$\dot{z}_v(x)=\frac{1}{v}\frac{\partial z(\frac{x}{v})}{\partial(\frac{x}{v})}=\frac{1}{v}\frac{\partial z(t)}{\partial(t)}=\frac{1}{v}\dot{z}(t); \tag{6}$$

Following the same approach, it can be shown that $\ddot{z}_v(x)=\frac{1}{v^2}\ddot{z}(t)$. Thus, the quarter car dynamics takes the form:

$$Mv^2\ddot{z_v}(x)+\xi v\dot{z_v}(x)+k(z_v(x)-z_r(x))=0. \tag{7}$$

To compute the cepstrum of the vertical acceleration of the vehicle, the analysis is moved to the Laplace domain. To this end, the transfer function between the vehicle's vertical displacement $Z_v(s)$ and the vertical displacement of the road profile $Z_r(s)$ is:

$$Z_v(s)=\frac{k}{Mv^2s^2+\xi vs+k}Z_r(s), \tag{8}$$

which implies that the transfer function between the vertical acceleration of the vehicle $Az_v(s)$, and the vertical displacement of the road $Z_r(s)$ is:

$$Az_v(s)=\frac{ks^2}{Mv^2s^2+\xi vs+k}Z_r(s). \tag{9}$$

The power spectrum of $Az_v(s)$, called $\phi_{Az_v}(\Omega)$ can be computed as:

$$\phi_{Az_v}(\Omega)=|F_v(j\Omega)|^2\cdot\phi_r(\Omega). \tag{10}$$

where:

$$F_v(j\Omega)=\frac{-k\Omega^2}{-Mv^2\Omega^2+\xi vj\Omega+k}. \tag{11}$$

The power spectral density associated with the vehicle's dynamic response is denoted as $\phi_{F_v}(\Omega)$, and takes the form of:

$$\begin{aligned}\phi_{F_v}(\Omega)&=|F_v(j\Omega)|^2\\&=\Big|\frac{-k\Omega^2}{-Mv^2\Omega^2+\xi vj\Omega+k}\Big|^2\\&=\Big(\frac{k}{Mv^2}\Big)^2\frac{\Omega^4}{\Big(\frac{k}{Mv^2}-\Omega^2\Big)^2+\Big(\frac{\Omega\xi}{Mv}\Big)^2}.\end{aligned}\tag{12}$$

In Equation (12), it is important to note that $\phi_{F_v}(\Omega)$ does not depend on the road profile $\phi_r(\Omega)$. In fact, it only depends on the vehicle parameters and the traveling speed v, which modulates the excitation of vehicle modes. On the other hand, as previously mentioned, $\phi_r(\Omega)$ does not depend on the traveling speed or the used vehicle, but only on the road surface profile.

This formulation highlights a common limitation of literature approaches that rely on spectral analysis. In fact, Equation (10) shows that the spectrum of the vertical acceleration measured by the onboard sensor can be expressed as the product of the road-related spectrum and the vehicle dynamic response. This implies that spectral features inherently reflect both the pavement condition and the specific vehicle–speed configuration, preventing a direct separation of these two contributions. Cepstral analysis, instead, enables the explicit separation of the vehicle-dependent term from the road-dependent one:

$$\begin{aligned}c_{Az_v}(q)&=\mathcal{F}^{-1}\{\log(\phi_{Az_v}(\Omega))\}\\&=\mathcal{F}^{-1}\{\log(\phi_{F_v}(\Omega))+\log(\phi_r(\Omega))\}\\&=c_{F_v}(q)+c_r(q).\end{aligned}\tag{13}$$

Notably, the contributions of the vehicle modes $c_{F_v}(q)$ and of the road surface quality $c_r(q)$, which are now separable thanks to the cepstrum properties. It follows that the core of the proposed approach consists of estimating the vehicle dynamics term, $c_{F_v}(q)$, given that the other quantities can be directly computed from the measured signals. In fact, once this term has been estimated, it becomes possible to obtain the road quality index $c_r(q)$ from Equation(13).

2.3 From Absolute to Relative Formulation

Equation (13) provides an absolute measure of the road quality, which poses significant challenges. In fact, it leads to estimates that are biased with respect to environmental conditions, to the specific vehicle, and road factors, which would require constant access to some form of ground truth for correction. Therefore, $c_r(q)$ is computed by normalizing it with respect to a high-quality road profile to be used as a reference. This choice not only makes the index formulation more robust, but also compliant with the regulation of many countries, which enforce a minimum acceptable quality level for different road types. Once the reference baseline is defined, it will be used to compute a relative pavement index. To do so, the previously derived equations are applied to a scenario in which two trials are conducted, with the same vehicle driven over two different road profiles, denoted as r_1 and r_2, each characterized by a different surface quality. For the sake of simplicity, let us assume that each trial is conducted at a constant but distinct speed values, i.e., $v_1\neq v_2$.

According to Equations 10 and 13, the power spectra of vertical acceleration signals measured during the two trials can be written as:

$$\begin{aligned}\phi_{Az_{v_1}}(\Omega)&=\phi_{F_{v_1}}(\Omega)\cdot\phi_{r_1}(\Omega),\\\phi_{Az_{v_2}}(\Omega)&=\phi_{F_{v_2}}(\Omega)\cdot\phi_{r_2}(\Omega).\end{aligned}\tag{14}$$

Also, their power cepstra are given by:

$$\begin{aligned}c_{Az_{v_1}}(q)&=c_{F_{v_1}}(q)+c_{r_1}(q),\\c_{Az_{v_2}}(q)&=c_{F_{v_2}}(q)+c_{r_2}(q).\end{aligned}\tag{15}$$

Since the inverse Fourier transform $\mathcal{F}^{-1}$ is a linear operator, one has:

$$\begin{aligned}c_{Az_{v_1}}(q)-c_{Az_{v_2}}(q)&=c_{F_{v_1}}(q)+c_{r_1}(q)-c_{F_{v_2}}(q)+c_{r_2}(q)\\&=c_{r_1}(q)-c_{r_2}(q)+c_{F_{v_1}}(q)-c_{F_{v_2}}(q).\end{aligned}\tag{16}$$

Also, recalling that, by definition, $c_{F_v}(q)=\mathcal{F}^{-1}\{\log(\phi_{F_v}(\Omega))\}$ and $\phi_{F_v}(\Omega)=|F_v(j\Omega)|^2$, (16) can be reformulated as:

$$\begin{aligned}c_{Az_{v_1}}(q)-c_{Az_{v_2}}(q)&=c_{r_1}(q)-c_{r_2}(q)\\&\quad+\mathcal{F}^{-1}\left\{\log\left(\frac{\phi_{F_{v_1}}(\Omega)}{\phi_{F_{v_2}}(\Omega)}\right)\right\}.\end{aligned}\tag{17}$$

Rearranging the terms, the difference in road surface qualities in the cepstral domain can be isolated, leading to the desired quality index:

$$c_{r_1}(q)-c_{r_2}(q)=c_{Az_{v_1}}(q)-c_{Az_{v_2}}(q)-\mathcal{F}^{-1}\left\{\log\left(\frac{\phi_{F_{v_1}}(\Omega)}{\phi_{F_{v_2}}(\Omega)}\right)\right\},\tag{18}$$

where $c_{r_2}(q)$ is the cepstra of the high-quality reference road profile.

2.4 Approximation of the Vehicle Dynamics Term

The only unknown component in (18) is $\mathcal{F}^{-1}\Big\{\log\Big(\frac{\phi_{F_{v_1}}(\Omega)}{\phi_{F_{v_2}}(\Omega)}\Big)\Big\}$, which accounts for the difference in vehicle dynamic response due to the speed change. However, as detailed in this subsection, with appropriate approximations, it can be reliably estimated from the collected data. To this end, the analysis starts from the definition of $\phi_{F_v}(\Omega)$ from Equation (12):

$$\begin{aligned}\frac{\phi_{F_{v_1}}(\Omega)}{\phi_{F_{v_2}}(\Omega)}&=\frac{\Big(\frac{k}{Mv_1^2}\Big)^2\frac{\Omega^4}{\Big(\frac{k}{Mv_1^2}-\Omega^2\Big)^2+\Big(\frac{\Omega\xi}{Mv_1}\Big)^2}}{\Big(\frac{k}{Mv_2^2}\Big)^2\frac{\Omega^4}{\Big(\frac{k}{Mv_2^2}-\Omega^2\Big)^2+\Big(\frac{\Omega\xi}{Mv_2}\Big)^2}}\\&=\Big(\frac{v_2}{v_1}\Big)^4\frac{\Big(\frac{k}{Mv_2{}^2}-\Omega^2\Big)^2+\Big(\frac{\Omega\xi}{Mv_2}\Big)^2}{\Big(\frac{k}{Mv_1{}^2}-\Omega^2\Big)^2+\Big(\frac{\Omega\xi}{Mv_1}\Big)^2}\\&=\frac{M^2v_2^4\Omega^4+(\xi^2-2kM)\Omega^2v_2^2+k^2}{M^2v_1^4\Omega^4+(\xi^2-2kM)\Omega^2v_1^2+k^2},\end{aligned}\tag{19}$$

which shows that both the numerator and the denominator are functions of the product Ωv. Accordingly, it can be noted that:

- For small values of Ωv, i.e.,
$$\Omega v\leq\sqrt{\frac{k^2}{|\xi^2-2kM|}},\tag{20}$$
$\phi_{F_v}(\Omega)$ can be approximated as $\phi_{F_v}(\Omega)\approx k^2$, making the overall ratio constant for different speed values.
- For medium-low values of Ωv, i.e.,
$$\sqrt{\frac{k^2}{|\xi^2-2kM|}}\leq\Omega v\leq\sqrt{\frac{k}{M}},\tag{21}$$
the $(\Omega v)^4$ can be considered negligible. Therefore
$$\phi_{F_v}(\Omega)\approx(\xi^2-2kM)\Omega^2v^2+k^2\approx m_a(\Omega)v^2.\tag{22}$$
Note that, for fixed spatial frequency Ω, $m_a(\Omega)$ is a function that can be learned from data.
- For medium-high values of Ωv, i.e.,
$$\sqrt{\frac{k}{M}}\leq\Omega v\leq\sqrt{\frac{|\xi^2-2kM|}{M^2}}\tag{23}$$
k^2 becomes negligible. Thus
$$\begin{aligned}\phi_{F_v}(\Omega)&\approx M^2\Omega^4v^4+(\xi^2-2kM)\Omega^2v^2\\&\approx\Omega^2v^2(M^2\Omega^2v^2+(\xi^2-2kM))\\&\approx m_b(\Omega)v^4\end{aligned}\tag{24}$$
where $m_b(\Omega)$ depends on Ω and vehicle parameters and can be estimated from data.

- Finally, for higher values of Ωv, when
$$\Omega v > \sqrt{\frac{|\xi^2 - 2kM|}{M^2}} \tag{25}$$
just the first term of $\phi_{F_v}(\Omega)$ must be considered, therefore $\phi_{F_v}(\Omega) \approx m_c(\Omega) v^4$.

Based on these approximations it is possible to say that the power spectral density of the vehicle dynamics, $\phi_{F_v}(\Omega)$, can be approximated as $\phi_{F_v}(\Omega) \approx m v^e$, where m and e depend on Ωv and specific vehicle parameters. Thus, letting:

- $\rho(\Omega) = m_2(\Omega)(m_1(\Omega))^{-1}$,
- $\gamma_1(\Omega) = -e_1(\Omega)$,
- $\gamma_2(\Omega) = -e_2(\Omega)$,

Equation (19) can be expressed as:
$$\frac{\phi_{F_{v_1}}(\Omega)}{\phi_{F_{v_2}}(\Omega)} \approx \frac{m_1(\Omega) \cdot v_1^{e_1(\Omega)}}{m_2(\Omega) \cdot v_2^{e_2(\Omega)}} = \rho(\Omega) \cdot \frac{v_1^{\gamma_1(\Omega)}}{v_2^{\gamma_2(\Omega)}}. \tag{26}$$

As detailed in Section 3, this result enables RPI to be computed from data, thanks to the ad-hoc designed one-time calibration procedure that allows us to estimate the required parameters. In fact, the ratio $\frac{\phi_{F_{v_1}}(\Omega)}{\phi_{F_{v_2}}(\Omega)}$ can be computed from vertical acceleration measurements, while the coefficients $\rho(\Omega)$,$\gamma_1(\Omega)$, and $\gamma_2(\Omega)$ can be also estimated from data. By substituting (26) into the logarithmic term used to compute the inverse Fourier transform, the following expression is obtained:
$$\log\left(\frac{\phi_{F_{v_1}}(\Omega)}{\phi_{F_{v_2}}(\Omega)}\right) = \log(\rho(\Omega)) + \gamma_1(\Omega)\log(v_1) + - \gamma_2(\Omega)\log(v_2), \tag{27}$$
making the formulation directly suitable for a linear regression approach, e.g., least squares.

2.5 RPI Formulation

Building upon the previous considerations, and especially Equation (27), (18) can be rewritten as:
$$c_{r_1}(q) - c_{r_2}(q) = c_{Az_{v_1}}(q) - c_{Az_{v_2}}(q) - \mathcal{F}^{-1}\{\log(\rho(\Omega)) + \gamma_1(\Omega)\log(v_1) - \gamma_2(\Omega)\log(v_2)\}, \tag{28}$$
From this formulation, considering the Martin distance to compute the cepstral difference, letting the road profile index $\Delta_{v_1,v_2}(q) = \mathcal{F}^{-1}\{\log(\rho(\Omega)) + \gamma_1(\Omega)\log(v_1) - \gamma_2(\Omega)\log(v_2)\}$, and assuming that the cepstrum of the vertical acceleration measured by the onboard accelerometer at speed v_2 over a reference high-quality road surface, flat and smooth, is negligible, i.e., $c_{r_2}(q) \approx 0$, RPI can be formulated as:
$$RPI = \sqrt{\sum_{q=0}^{Q} q |c_{Az_{v_1}}(q) - c_{Az_{v_2}}(q) - \Delta_{v_1,v_2}(q)|^2}, \tag{29}$$
where Q is the cepstral order. Note that higher RPI values indicate poorer road quality. Therefore, assuming that $c_{Az_{v_1}}(q)$, $c_{Az_{v_2}}(q)$, and $\Delta_{v_1,v_2}(q)$ can be calculated from the data, the presented formulation yields an estimate of the quality of the road profile that is independent of the vehicle dynamics and, as will be shown later, independent of vehicle speed.

3. ALGORITM DESIGN

As discussed in Section 2, to provide a real-time accurate estimation of the road quality according to the RPI definition, the parameters $\rho(\Omega)$,$\gamma_1(\Omega)$, and $\gamma_2(\Omega)$ of the $\Delta_{v_1,v_2}(q)$ function, and the terms of $c_{Az_{v_2}}(q)$ must be learned. The latter consists of the cepstrum of the vertical acceleration measured by the onboard accelerometer when the vehicle is driven at speed v_2 over a reference high-quality road surface, which, as previously noted, can be approximated as $c_{r_2}(q) \approx 0$. Once these parameters are learned, Equation (29) can be applied to provide road-quality estimates.

Delving into the details of the approach, the first stage is divided into two steps: one dedicated to the identification of $\Delta_{v_1,v_2}(q)$ parameters, and the other aimed at computing $c_{Az_{v_2}}(q)$. It is important to note that these parameters need to be estimated only once and offline for each new vehicle, to be then used online at prediction time, and that the speed v_2 must be the same in the two stages. To perform the first stage of the learning process, i.e., to estimate $\Delta_{v_1,v_2}(q)$, several trials must be performed at different constant speeds on road segments of similar quality (e.g., highway–highway, urban-urban). If this requirement is satisfied, it can be assumed that the difference of the road cepstra is negligible, i.e., $c_{r_1}(q) - c_{r_2}(q) \approx 0$, since the road geometry is the same. Thus Equation (17) becomes:
$$c_{Az_{v_1}}(q) - c_{Az_{v_2}}(q) = \Delta_{v_1,v_2}(q) = \mathcal{F}^{-1}\left\{\log\left(\frac{\phi_{F_{v_1}(\Omega)}}{\phi_{F_{v_2}}(\Omega)}\right)\right\}. \tag{30}$$
This result is key, as it indicates that $c_{Az_{v_1}}(q) - c_{Az_{v_2}}(q)$, that is, the cepstral distance computed from the vertical acceleration measured during the trials, corresponds to the value $\Delta_{v_1,v_2}(q)$. In turn, by computing the power spectrum of the measured accelerations in a segment of the same length traveled at different speeds, i.e., v_1 and v_2, it results:
$$\log\left(\frac{\phi_{Az_1}(\Omega)}{\phi_{Az_2}(\Omega)}\right) = [\log(\rho(\Omega)) + \gamma_1(\Omega)\log(v_1) - \gamma_2(\Omega)\log(v_2)]. \tag{31}$$
Expressing this equation in vectorized form, with ϕ_{Az_1} and ϕ_{Az_2} containing the spectral coefficients computed at speed v_1 and v_2, and the three parameter vectors $\rho(\Omega)$, $\gamma_1(\Omega)$ and $\gamma_2(\Omega)$, a least square problem can be set as:
$$\underbrace{\log(\Phi_{Az_1} \oslash \Phi_{Az_2})}_{\mathbf{y}} = \underbrace{\gamma_1 \log(v_1) - \gamma_2 \log(v_2)}_{\mathbf{Ax}} + \underbrace{\log(\rho)}_{\mathbf{b}}. \tag{32}$$
Please note that in this formulation $y \in \mathbb{R}^{N \times 1}$, $A \in \mathbb{R}^{N \times 2}$, $b \in \mathbb{R}^{N \times 1}$, and $x \in \mathbb{R}^{2 \times 1}$, where N is the size of the vector of spatial frequency values Ω. Thanks to this process, for each frequency up to the chosen spatial resolution, estimates of $\rho(\Omega)$, $\gamma_1(\Omega)$, and $\gamma_2(\Omega)$ are obtained. As reported in Section 2, this result implies that the learned parameters characterize the vehicle's dynamic response and are valid regardless of the road surface and the traveling speed.

Letting $v_1 = v_{new}$ be the vehicle's traveling speed at inference time and $v_2 = v_{ref}$ the reference speed used during the learning phase, which means that $\Delta_{v_{new},v_{ref}} = \mathcal{F}^{-1}\{[\log(\rho(\Omega)) + \gamma_1(\Omega)\log(v_{new}) - \gamma_2(\Omega)\log(v_{ref})]\}$. Accordingly, assuming that the power spectrum of the vertical acceleration measured at the reference speed v_{ref} is available, RPI can be computed according to (29). To improve the robustness of the identified parameters, it is recommended to performing multiple trials on the same road at different speeds, and then segmenting each trial into shorter windows over which the speed can be assumed approximately constant. Empirically, it can be noted that, considering $100m$ windows, this assumption can be verified by keeping only the windows in which the speed variance σ^v is below 2.5 km/h. The window size was fine-tuned to ensure stationarity while preserving enough signal dynamics for meaningful Fourier Transform computation. Please note that, as these parameters characterize the intrinsic dynamic response of the vehicle, they need to be estimated only once. Once identified, these parameters can be reliably used for online RPI estimation under arbitrary speed profiles. In this regard, it is important to note that the constant-speed assumption mentioned in Section 2 is required only locally. In practice, the collected signals are segmented into short spatial windows within which the vehicle speed can be considered approximately constant. For the same reason, even real-time RPI computation

does not require globally constant speed, but only local quasi-stationarity, which is fully compatible with naturalistic driving conditions. According to (29), the second parameter that needs to be estimated in the learning phase is the cepstrum of the overall vertical acceleration signal at speed v_{ref}. To this end, a series of trials must be conducted using the same vehicle, traveling at a reference speed v_{ref}, over road segments that meet standards of sufficiently high quality to be considered as reference, e.g., highways that must have a minimum roughness level for safety reasons, with periodic maintenance enforced by law. Accordingly, the power cepstrum of the reference measured vertical acceleration, $c_{Az_{v_{ref}}}(q)$, can be computed as:

$$c_{Az_{v_{ref}}}(q) = \mathcal{F}^{-1}\{\log(\phi_{Az_{v_{ref}}}(\Omega))\}, \tag{33}$$

where $\phi_{Az_{v_{ref}}}(\Omega)$ is the power spectrum of the measured vertical acceleration signal. However, since highway pavement quality may still exhibit variability, computing regularized cepstra should be preferred, obtained by considering the average power spectrum across several non-overlapping segments. Specifically, considering N_l learning windows available, which in this case are 100 m long, this power spectrum is:

$$\overline{\phi}_{Az_{v_{ref}}}(\Omega) = \frac{1}{N_l}\sum_{n=1}^{N_l}\phi_{Az_{v_{ref},n}}(\Omega), \tag{34}$$

where $\phi_{Az_{v_{ref},n}}(\Omega)$ is the power spectrum computed in the n_{th} learning window. Once the learning phase is completed, the prediction phase is straightforward. In fact, for each new trial, sliding windows of the same length used in the learning phase are considered, 100 m, and the RPI is computed using (29).

4. EXPERIMENTAL RESULTS AND DISCUSSION

To validate the proposed algorithm in real-world conditions, an experimental campaign was conducted with two vehicles—a Mercedes-Benz B-Class and a Fiat Panda 4WD—and different drivers, selected to cover diverse size, mass, and handling characteristics. Both vehicles were equipped with a MetaSystem T31.2 e-box, powered by the vehicle battery, providing all measurements required for RPI: an IMU (tri-axial accelerometer and gyroscope at 400 Hz) and a GPS/GNSS module (10 Hz) for geolocation, speed, and distance. Data were collected on road segments with homogeneous but different quality, traveled by both vehicles within a short time window, totaling about 100 km per vehicle. Specifically, each vehicle covered approximately 6 km of off-road (unpaved rural roads), 25 km of urban roads (generally good with local irregularities), and 80 km of highways (high-quality by design). Driving was mostly naturalistic, with reference speeds of 85 km/h and 95 km/h maintained long enough for parameter estimation. For each vehicle, the 70% of the data collected in the highway scenario has been used for learning purposes, i.e., to identify $\rho(\Omega)$, $\gamma_1(\Omega)$, and $\gamma_2(\Omega)$. The remaining data, including unused portions of highway trials as well as off-road and urban segments, was employed for validation. After the split, learning and validation data were both segmented into non-overlapping windows of 100 meters. Then, according to the algorithm reported in Section 3, only those in which the vehicle speed standard deviation was below 2.5 km/h were considered, to enforce constant-speed conditions. Accordingly, less than 1% of the data was excluded. The signal has then been resampled with respect to the spatial domain. Once the dataset was curated, the vehicle parameters could be learned.

Specifically, the learning phase consists of the following:

(1) Estimate the functions $\rho(\Omega)$, $\gamma_1(\Omega)$, and $\gamma_2(\Omega)$ via least squares regression (32).
(2) Compute $c_{Az_{v_{ref}}}(q)$, according to (33).

Then, the identified parameters are used to compute RPI online for each new window in the validation dataset by evaluating (29). Therefore, it can be noted that, since the online RPI prediction only requires spectrum and cepstrum estimation and the evaluation of closed-form expressions, the computational burden is low and compatible with real-time deployment. The resulting RPI distributions for each road surface are reported in Figure 1. Before analyzing the results, it is worth noting that the presented analysis is not intended as a classification pipeline, but as an a posteriori assessment. Specifically, the aim is to verify that road quality indicator distributions across the three terrains are statistically distinguishable, regardless of vehicle and speed. These results demonstrate the effectiveness of the proposed index, showing that RPI produces consistent values regardless of vehicle speed and dynamic behavior, thereby confirming its robustness and reliability.

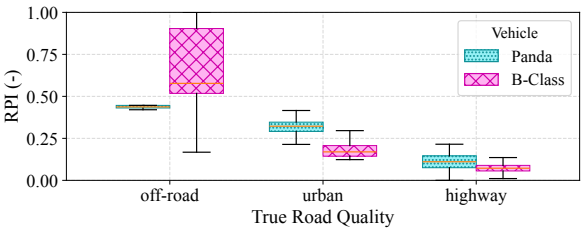


Fig. 1. Aggregated distribution of RPI in the validation dataset.

To further demonstrate the effectiveness of the proposed index, it has been compared with alternative formulations. To this end, an ablation study has first been performed to prove the need for each of the debias terms included. To this end, always considering validation data, three indices have been evaluated:

- $RPI_{road} = \sqrt{\sum_{q=0}^{Q} q|c_{Az_{v_{new}}}(q) - c_{Az_{v_{ref}}}(q)|^2}$.
  This formulation only accounts for the bias due to the reference road surface;
- $RPI_{vehicle} = \sqrt{\sum_{q=0}^{Q} q|c_{Az_{v_{new}}}(q) - \Delta_{v_{new},v_{ref}}(q)|^2}$.
  This formulation only accounts for the bias due to the vehicle dynamics at different speed;
- $RPI_{none} = \sqrt{\sum_{q=0}^{Q} q|c_{Az_{v_{new}}}(q)|^2}$.
  This formulation does not account for any bias compensation.

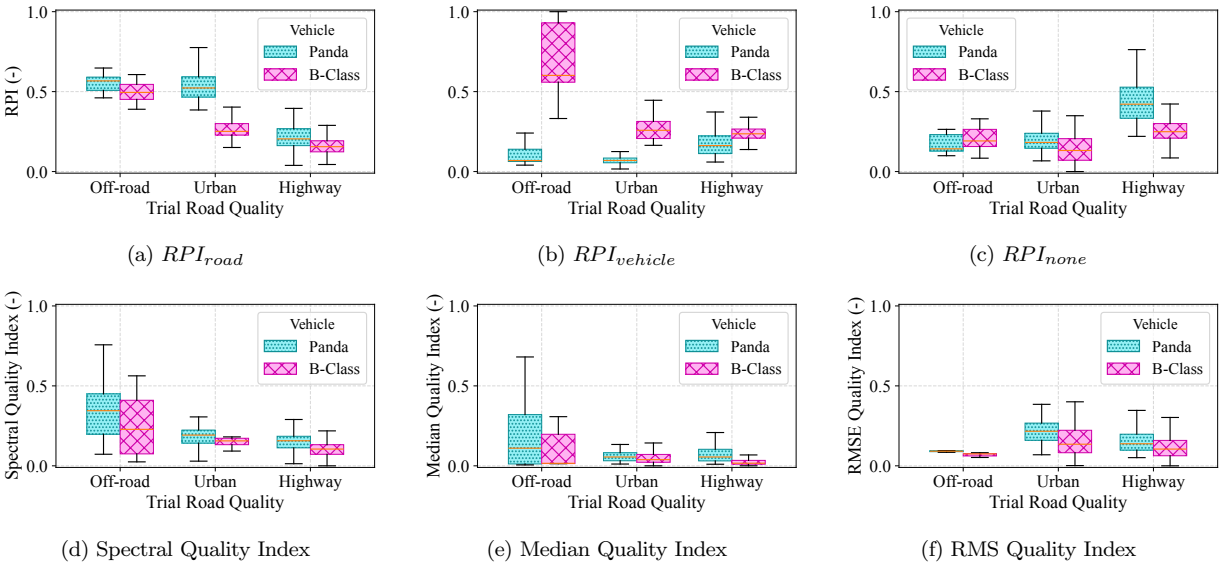
In addition, the proposed index has been compared with three common counterparts from the literature that rely on the same sensor setup. As discussed in Section 1, these indices typically focus on the energy content of the vertical acceleration signal, analyzed either in the frequency or in the time domain. To this end, an index based on the power spectrum of the vertical acceleration signal has first been computed, defined as the Spectral Quality Index. Inspired by Leoni et al. (2023) and the traditional IRI formulation, this index has been formulated as:

$$SpectralQualityIndex = \\ = \sqrt{|Area[\phi_{Az_{new}}(\Omega)] - Area[\phi_{Az_{ref}}(\Omega)]|},$$

where $Area[\phi_{Az_n}]$ is the area under the power spectrum of the signal, representing its energy content. Also, the formulation proposed in Wage and Sester (2021) has been evaluated, which is based on the median of the vertical acceleration in a specific window of data. According to its definition, this index, defined as Median Quality Index, has been computed as:

$$MedianQualityIndex = \frac{MAD(t)}{5\tilde{v}} \tag{35}$$

where $MAD(t) = \text{median}\left(|Az(t) - \tilde{Az}|\right)$, and $\tilde{Az}$ and $\tilde{v}$ are the median vertical acceleration and the median vehicle speed in the window, respectively. Last, the formulation in Zeng et al. (2018) has been taken into account, which defines the roughness



(a) RPI_{road} (b) $RPI_{vehicle}$ (c) RPI_{none}

(d) Spectral Quality Index (e) Median Quality Index (f) RMS Quality Index

Fig. 2. Aggregated distribution of the ablated version of the proposed RPI and of the literature index formulations.

index as the RMS of the vertical acceleration signal within a window W:

$$RMSQualityIndex = \sqrt{\frac{1}{W}\int_0^W Az^2(t)dt}. \tag{36}$$

The objective of these analyses is to evaluate the ability of each index to provide values that are consistent with the actual road quality of the test, while being consistent with changing vehicle and traveling speed. Therefore, the index distribution with respect to terrain and vehicle has been investigated. The results are shown in Figure 2. RPI values are normalized in [0,1] for comparison, without vehicle-specific scaling to avoid compensating vehicle-induced biases.

The ablation study shows that the proposed RPI outperforms all alternatives, which are affected by biases from vehicle dynamics and speed. For instance, RPI_{road} correctly assigns low values to highways but fails to distinguish urban and off-road segments, with strong influence from vehicle dynamics. Similarly, $RPI_{vehicle}$ removes speed-related effects but remains biased by vehicle type, while RPI_{none} is highly inaccurate, even misclassifying highways as worse due to higher speeds. Among alternative indices, the Spectral Quality Index follows the expected trend but exhibits high variance and strong vehicle dependence, highlighting limitations of frequency-based and machine learning approaches. The Median Quality Index shows weak class separation and high variability, as it does not compensate for speed and vehicle dynamics. The RMS Quality Index, being time-domain, is strongly affected by speed, often increasing for urban and highway segments due to higher velocities, leading to biased estimates. Overall, these results confirm that time-domain metrics coupled with speed fail to reliably discriminate road quality.

5. CONCLUDING REMARKS

This work proposes a novel roughness index, RPI, designed to be independent of vehicle dynamics and speed. Using cepstral analysis of vertical acceleration, it decouples vehicle modes from road quality without requiring prior knowledge of vehicle parameters, relying instead on a one-time calibration. This makes the method scalable, simple, and cost-effective. Experimental validation on naturalistic drives with different vehicles shows consistent results across speeds. Future work will assess robustness on larger fleets, including heavy-duty vehicles, and investigate higher-order vehicle models.

REFERENCES

Bogert, B.P. (1963). The quefrency alanysis of time series for echoes: Cepstrum, pseudoautocovariance, cross-cepstrum and saphe cracking. In *Proceedings of Symposium Time Series Analysis, 1963*, 209–243.

Bonnardot, F. (2019). Influence of speed fluctuation on cepstrum. *Mechanical Systems and Signal Processing*, 119, 81–99. doi:10.1016/j.ymssp.2018.09.010.

Braghin, F., Cheli, F., Melzi, S., and Resta, F. (2006). Tyre wear model: validation and sensitivity analysis. *Meccanica*, 41, 143–156. doi:10.1007/s11012-005-1058-9.

Leoni, J., Lucchini, A., Strada, S.C., Tanelli, M., and Savaresi, S.M. (2023). Active driver assistance systems for e-scooters based on road quality and driving style estimation. *IFAC-PapersOnLine*, 56(2), 1977–1982. doi:10.1016/j.ifacol.2023.10.1091.

Loprencipe, G., Zoccali, P., and Cantisani, G. (2019). Effects of vehicular speed on the assessment of pavement road roughness. *Applied Sciences*, 9(9), 1783. doi:doi.org/10.3390/app9091783.

Martin, R.J. (2002). A metric for arma processes. *IEEE transactions on Signal Processing*, 48(4), 1164–1170. doi:10.1109/78.827549.

Randall, R.B. (2017). A history of cepstrum analysis and its application to mechanical problems. *Mechanical Systems and Signal Processing*, 97, 3–19. doi:10.1016/j.ymssp.2016.12.026.

Spangler, E.B. and Kelly, W.J. (1965). Gmr road profilometer-a method for measuring road profile. *Highway Research Record*, 121, 27–54.

Wage, O. and Sester, M. (2021). Joint estimation of road roughness from crowd-sourced bicycle acceleration measurements. *ISPRS Annals of the Photogrammetry Remote Sensing and Spatial Information Sciences*, 89–96. doi:10.5194/isprs-annals-V-4-2021-89-2021.

Yiliguoqi, B., Siriguleng, B., Arong, Guo, G., and Wang, J. (2026). Research on the evaluation and analysis of road surface roughness based on smartphone sensors and svm. *Scientific Reports*. doi:10.1038/s41598-025-34396-3.

Zeng, H., Park, H., Smith, B.L., and Parkany, E. (2018). Feasibility assessment of a smartphone-based application to estimate road roughness. *KSCE Journal of Civil Engineering*, 22(8), 3120–3129. doi:10.1007/s12205-017-1008-9.

Zhang, Q., Hou, J., Hu, X., Yuan, L., Jankowski, Ł., An, X., and Duan, Z. (2022). Vehicle parameter identification and road roughness estimation using vehicle responses measured in field tests. *Measurement*, 199, 111348.